(12) INTERNATIONAL APPLICATION PUBLISHED UNDER THE PATENT COOPERATION TREATY (PCT)

(19) World Intellectual Property Organization

International Bureau





(10) International Publication Number WO 2017/155655 A1

(43) International Publication Date 14 September 2017 (14.09.2017)

(51) International Patent Classification: G01V 1/30 (2006.01) G01V 1/22 (2006.01) G01V 1/24 (2006.01)

(21) International Application Number:

PCT/US2017/017082

(22) International Filing Date:

9 February 2017 (09.02.2017)

(25) Filing Language:

English

(26) Publication Language:

English

(30) Priority Data:

1652041 11 March 2016 (11.03.2016) FR

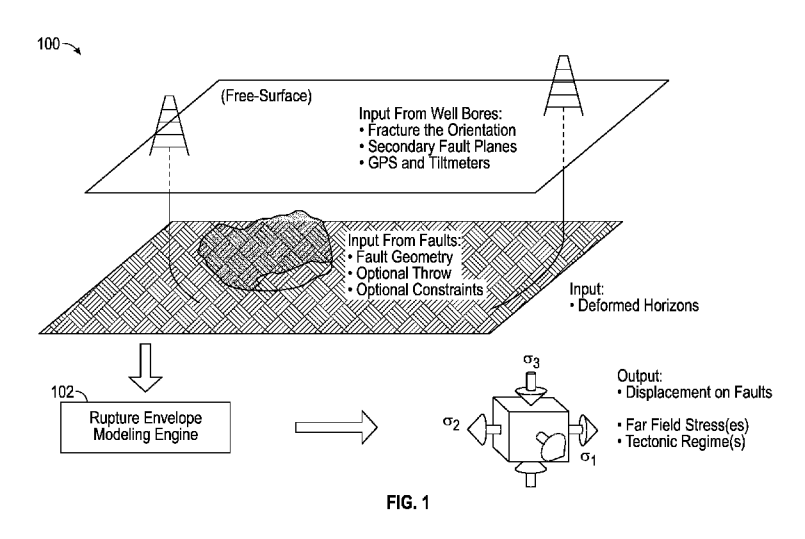
- (71) Applicant (for US only): SCHLUMBERGER TECHNO-LOGY CORPORATION [US/US]; 300 Schlumberger Drive, Sugar Land, Texas 77478 (US).
- (71) Applicant (for CA only): SCHLUMBERGER CANADA LIMITED [CA/CA]; 125 - 9 Avenue SE, Calgary, Alberta T2G 0P6 (CA).
- (71) Applicant (for FR only): SERVICES PETROLIERS 75007 Paris (FR).
- (71) Applicant (for all designated States except CA, FR, US): GEOQUEST SYSTEMS B.V. [NL/NL]; Gevers Deynootweg 61, 2586 BJ The Hague (NL).
- Inventors: MAERTEN, Frantz; c/o Parc Industriel et Technologique de la Pompignane, Schlumberger MpTC,

895 Rue de la Vieille Poste, 34006 Montpellier (FR). MAERTEN, Laurent; c/o Schlumberger MpTC, Parc Industriel et Technologique de la Pompignane, 895 Rue de la Vieille Poste, 34006 Montpellier (FR). JOONNEKINDT, Jean Pierre; c/o Schlumberger MpTC, Parc Industriel et Technologique de la Pompignane, 895 Rue de la Vieille Poste, 34006 Montpellier (FR).

- Agents: WIER, Colin L. et al.; 10001 Richmond Avenue, Houston, Texas 77042 (US).
- (81) Designated States (unless otherwise indicated, for every kind of national protection available): AE, AG, AL, AM, AO, AT, AU, AZ, BA, BB, BG, BH, BN, BR, BW, BY, BZ, CA, CH, CL, CN, CO, CR, CU, CZ, DE, DJ, DK, DM, DO, DZ, EC, EE, EG, ES, FI, GB, GD, GE, GH, GM, GT, HN, HR, HU, ID, IL, IN, IR, IS, JP, KE, KG, KH, KN, KP, KR, KW, KZ, LA, LC, LK, LR, LS, LU, LY, MA, MD, ME, MG, MK, MN, MW, MX, MY, MZ, NA, NG, NI, NO, NZ, OM, PA, PE, PG, PH, PL, PT, QA, RO, RS, RU, RW, SA, SC, SD, SE, SG, SK, SL, SM, ST, SV, SY, TH, TJ, TM, TN, TR, TT, TZ, UA, UG, US, UZ, VC, VN, ZA, ZM, ZW.
- SCHLUMBERGER [FR/FR]; 42 rue Saint Dominique, (84) Designated States (unless otherwise indicated, for every kind of regional protection available): ARIPO (BW, GH, GM, KE, LR, LS, MW, MZ, NA, RW, SD, SL, ST, SZ, TZ, UG, ZM, ZW), Eurasian (AM, AZ, BY, KG, KZ, RU, TJ, TM), European (AL, AT, BE, BG, CH, CY, CZ, DE, DK, EE, ES, FI, FR, GB, GR, HR, HU, IE, IS, IT, LT, LU, LV, MC, MK, MT, NL, NO, PL, PT, RO, RS, SE, SI, SK,

[Continued on next page]

(54) Title: DETERMINING RUPTURE ENVELOPES OF A FAULT SYSTEM



(57) Abstract: Provided are a method, computer-readable medium, and a system for determining rupture envelopes for a fault system. The method includes obtaining a representation that depicts one or more faults in a region of the earth as triangulated surfaces; selecting variables from among parameters comprising stress ratio, orientation of far field stress maximum principal stress, intermediate principal stress, minimum principal stress for the far field stress, and sliding friction and cohesion of the fault system; determining a strain energy of a triangular element based on a friction coefficient, a normal stress on the triangular element, and a cohesion for the variables; summing the strain energy of each triangle in the triangulated surfaces to yield an effective shear strain energy; extracting one or more iso-surfaces of the effective shear strain energy based on the summing; and creating rupture envelopes for specific values of the effective shear strain energy.



SM, TR), OAPI (BF, BJ, CF, CG, CI, CM, GA, GN, GQ, Published: GW, KM, ML, MR, NE, SN, TD, TG).

— with it

— with international search report (Art. 21(3))

DETERMINING RUPTURE ENVELOPES OF A FAULT SYSTEM

Background

[0001] A fault may be considered a finite complex three-dimensional surface discontinuity in a volume of earth or rock. Fractures, including, without limitation, joints, veins, dikes, pressure solution seams with stylolites, and so forth, may be propagated intentionally, to increase permeability in formations such as shale, in which optimizing the number, placement, and size of fractures in the formation increases the yield of resources like shale gas.

[0002] Stress, in continuum mechanics, may be considered a measure of the internal forces acting within a volume. Such stress may be defined as a measure of the average force per unit area at a surface within the volume on which internal forces act. The internal forces may be produced between the particles in the volume as a reaction to external forces applied to the volume.

[0003] Understanding the origin and evolution of faults and the tectonic history of faulted regions can be accomplished by relating fault orientation, slip direction, geologic and geodetic data to the state of stress in the earth's crust. In certain inverse problems, the directions of the remote principal stresses and a ratio of their magnitudes are constrained by analyzing field data on fault orientations and slip directions as inferred from artifacts such as striations on exposed fault surfaces. Also, even if many faults surfaces can be interpreted from seismic, for a given geological time, some of them were active (i.e., were not sealed) and therefore have slipped. Since slipping faults greatly perturbed the stress, and consequently generate associated fracturation, it may be desirable to determine, for a given geological time (past or present), which faults were active and which were sealed (i.e., inactive).

[0004] Conventionally, a numerical code, such as a fine element method or a boundary element method, is used to determine a slip/no-slip condition of a fault system, which is used for the extraction of other rupture envelopes. However, these conventional methods have had certain limitations.

Summary

[0005] In accordance with examples of the present disclosure, a method, a computer-readable medium, and a system operable to execute the method for determining rupture envelopes for a

fault system. The method can include obtaining a representation that depicts one or more faults in a region of the earth as triangulated surfaces; selecting variables from among parameters comprising stress ratio, orientation of far field stress maximum principal stress, intermediate principal stress, minimum principal stress for the far field stress, and sliding friction and cohesion of the fault system; determining a strain energy of a triangular element based on a friction coefficient, a normal stress on the triangular element, and a cohesion for the variables; summing the strain energy of each triangle in the triangulated surfaces to yield an effective shear strain energy; extracting one or more iso-surfaces of the effective shear strain energy based on the summing; and creating one or more rupture envelopes for specific values of the effective shear strain energy based on the extracting.

[0006] In accordance with examples of the present disclosure, the representation is a three-dimensional representation and wherein the variables comprises a triplet of variables.

[0007] In accordance with examples of the present disclosure, the method includes causing the one or more rupture envelopes to be displayed.

[0008] In accordance with examples of the present disclosure, the determining the strain energy of the triangular element comprises using a Mohr-Coulomb criterion given by the equation $\mu\sigma_n + C_0$, wherein μ is the friction coefficient, σ_n normal stress on a triangular element, and C_0 is the cohesion.

[0009] In accordance with examples of the present disclosure, the method further includes determining a projection of a stress tensor on a crack plane and a projection of the stress tensor normal of the crack plane.

[0010] In accordance with examples of the present disclosure, the representation is obtained based at least in part on field data, wherein the field data includes multiple types of geologic data obtained from multiple sources, comprising one of seismic interpretation data, well bore data, or field observation data; and wherein the multiple types of geologic data comprise one of fault geometry data, fault throw data, slickenline data, displacement data for a geologic fault.

[0011] In accordance with examples of the present disclosure, the one or more iso-surfaces are extracted using a marching cube graphics algorithm.

[0012] In accordance with examples of the present disclosure, the effective shear strain energy of a value close to zero corresponds to a transition between slip and no-slip for a fault.

[0013] In accordance with examples of the present disclosure, the strain energy is based on difference between a projection of a stress tensor on a crack plane (" τ ") and a Mohr-Coulomb criterion, if the τ is greater than the Mohr-Coulomb criterion.

[0014] In accordance with examples of the present disclosure, the effective shear strain energy is the sum from all triangular elements of the individual strain energy.

[0015] In accordance with examples of the present disclosure, a transition between slip and noslip for a fault is characterized by a transition between the effective shear strain energy between zero and non-zero.

[0016] It will be appreciated that this summary is intended merely to introduce some aspects of the present methods, systems, and media, which are more fully described and/or claimed below. Accordingly, this summary is not intended to be limiting.

Brief Description of the Drawings

[0017] The accompanying drawings, which are incorporated in and constitute a part of this specification, illustrate embodiments of the present teachings and together with the description, serve to explain the principles of the present teachings. In the figures:

[0018] FIG. 1 is a diagram of an example stress, fracture, and fault activity modeling system;

[0019] FIG. 2 is a block diagram of an example computing environment for performing stress, fracture, and fault activity modeling using the principle of superposition;

[0020] FIG. 3 is an example method for computing rupture envelopes, according to examples of the present disclosure;

[0021] FIG. 4 shows an example representation of a plane with its normal \bar{n} ;

[0022] FIG. 5 shows graphical convention used for the following examples;

[0023] FIGS. 6A and 6B illustrate an example rupture envelope for a planar fault and associated triangulated surface, respectively, according to examples of the present disclosure;

[0024] FIGS. 7A and 7B illustrate an example rupture envelope for a spherical fault and associated triangulated surface, respectively, according to examples of the present disclosure;

[0025] FIGS. 8A and 8B illustrate an example rupture envelope for two branching faults at 30° and associated triangulated surface, respectively, according to examples of the present disclosure;

[0026] FIGS. 9A and 9B illustrate an example rupture envelope for two branching faults at 90° and associated triangulated surface, respectively, according to examples of the present disclosure;

[0027] FIGS. 10A and 10B illustrate an example rupture envelope for two branching faults at 120° and associated triangulated surface, respectively, according to examples of the present disclosure;

[0028] FIGS. 11A and 11B illustrate an example rupture envelope for salt domes and associated triangulated surface, respectively, according to examples of the present disclosure;

[0029] FIGS. 12A and 12B illustrate an example rupture envelope for a complex fault system and associated triangulated surface, respectively, according to examples of the present disclosure; and

[0030] FIGS. 13A and 13B illustrate an example rupture envelope for another complex fault system and associated triangulated surface, respectively, according to examples of the present disclosure.

Detailed Description

[0031] The following detailed description refers to the accompanying drawings. Wherever convenient, the same reference numbers are used in the drawings and the following description to refer to the same or similar parts. While several embodiments and features of the present disclosure are described herein, modifications, adaptations, and other implementations are possible, without departing from the spirit and scope of the present disclosure.

[0032] DEFINITIONS

[0033] In the description below, certain variables are used in order to simplify the presentation. Table 1 below shows each variable that may be used and the variables' corresponding definition in accordance with examples of the present disclosure.

[0034] Table 1 - Parameters used to define the new criterion:

1.	Sliding friction coefficient for the micro cracks:	μ
2.	Cohesion of the micro cracks:	C_{o}
3.	Orientation of the far field stress:	θ
4.	Stress ratio defined as $(\sigma_2 \sigma_3)/(\sigma_1 \sigma_3)$ and $\in [0,1]$:	\overline{R}
5.	Maximum principal stress:	σ_1
6.	Intermediate principal stress:	σ_2
7.	Minimum principal stress:	σ_3

[0035] Effective shear stress (noted τ_{eff}): the difference between the resolve shear stress onto the triangular element and the Mohr-Coulomb criterion: $\tau_{eff} = \tau$ M_c if τ >Mc, 0 otherwise.

[0036] Strain energy for triangular element: the effective shear stress gives rise to the strain energy: $W_e = a \cdot \tau_{eff}^2$ (a is a constant for a given material)

[0037] Effective shear strain energy: the sum of all strain energy for a surface made of multiple triangular elements.

In accordance with examples of the present disclosure, a method and associated system, and computer readable medium operate to execute the method of determining the stability of a fault system subjected to tectonic constraints and fluid pressure is provided. In particular, given a system composed of one to many triangulated faults surfaces in 3D, the stability of the fault system is determined, at least in part, on the transition between a slip and a no-slip condition given a friction law on the fault surfaces. By varying the tectonic constraint as well as the parameters of the friction law (e.g., friction and/or cohesion), rupture envelopes are built in 3D which tells when the fault system will start to slip. A rupture envelope, also called a failure envelope, is the locus of all shear and normal stresses at failure for a given rock material. A failure envelope delineates stable and unstable states of stress for a given rock material. Using the Coulomb criterion for sliding faults, as discussed below, the first rupture envelope corresponds to the effective shear strain energy equals to zero. Using the Coulomb criterion for sliding faults as discussed below, additional failure envelopes corresponding to the value of the effective shear strain energy produced by the sliding fault surfaces can be generated. tectonic constraints are the parameters defining the far field stress (or tectonic stress) applied to the model as boundary condition. For Andersonian stress field, it is two parameters such as θ , the orientation of the principal horizontal stress according to the north, and R, the stress ratio, $R = (\sigma_2 \quad \sigma_3)/(\sigma_1 \quad \sigma_3)$. Rupture envelopes corresponding to the transition of slip/no-slip can be computed based on the effective shear strain energy. The effective shear strain energy can also be used to compute rupture envelopes corresponding to a specific values of the effective shear strain energy of a fault system, which can be compared to a specific geomechanical parameter of the fault system.

[0039] FIG. 1 shows an example stress, fracture, and fault activity modeling system 100. The example system 100 may be capable of solving a variety of geomechanical problems. The faults geometry may be known (and optionally, imposed inequality constraints such as normal, thrust,

etc., may be known), and fault activity (active faults versus inactive faults) of certain faults may be known. The user may have access to one or more of data from well bores (e.g., fracture orientation, in-situ stress measurements, secondary fault planes), geodetic data (e.g., InSAR, GPS, and tilt-meter), and/or as interpreted horizons. An example rupture envelope modeling engine 102 and/or corresponding example methods can determine one or more rupture envelopes (or yield surfaces) corresponding to a specific values of the effective shear strain energy of a fault system.

[0040] FIG. 2 shows the example system 100 of FIG. 1 in the context of a computing environment in which rupture envelopes of a fault system can be performed. The computing device 200 may be a computer, computer network, or other device that has a processor 208, memory 210, data storage 212, and other associated hardware such as a network interface 214 and a media drive 216 for reading and writing a removable storage medium 218. The removable storage medium 218 may be, for example, a compact disc (CD); digital versatile disk/digital video disc (DVD); flash drive, etc. The removable storage medium 218 contains instructions, which when executed by the computing device 200, cause the computing device 200 to perform one or more example methods described herein. Thus, the removable storage medium 218 may include instructions for implementing and executing the example rupture envelopes using engine 102 and/or graphical display etc. Specifically, software instructions or computer readable program code to perform embodiments may be stored, temporarily or permanently, in whole or in part, on a non-transitory computer readable medium such as a CD, a DVD, a local or remote storage device, local or remote memory, a diskette, or any other computer readable storage device.

[0041] In this example system, the computing device 200 receives incoming data 220, such as faults geometry and many other kinds of data, from multiple sources, such as well bore measurements 222, field observation 224, and seismic interpretation 226 from, for example, a subsurface earth volume 202, reservoir 204, and associated wells 206. The computing device 200 can receive one or more types of data sets 220 via the network interface 214, which may also receive data from a network (e.g., the Internet 228), such as GPS data and InSAR data.

The computing device 200 may compute (or calculate) and compile modeling results, simulator results, and control results, and a display controller 230 may output geological model images and simulation images and data to a display 232. The images may be 2D or 3D representations 234

of the one or more rupture envelopes generated by rupture envelope modeling engine 102, which may also generate one or more visual user interfaces (UIs) for input and/or display of data.

[0042] Rupture envelope modeling engine 102 may also generate or ultimately produce control signals to control field operations associated with the subsurface volume. For example, the field operations may be performed using drilling and exploration equipment, well control injectors and valves, or other control devices in real-world control of the reservoir 204, transport and delivery network, surface facility, and so forth. The one or more rupture envelopes can also be use to estimate the risk of reactivated a fault system.

[0043] Thus, an example system 100 may include a computing device 200 and interactive graphics display unit 232. The computing environment of the example system 100 as a whole may constitute simulators and models.

[0044] FIG. 3 shows an example method for calculating rupture envelopes, according to examples of the present disclosure. The method 300 begins at 302. At 304, a representation of a fault system is obtained. As discussed above, the fault system can be stored in memory 210 and can be modeled using modeling engine 102. The fault system can be represented in 3D and can be obtained based at least in part on field data. The field data can include one or more of multiple types of geologic data obtained from multiple sources, such as diverse data 220, including one of seismic interpretation data, well bore data, or field observation data; and wherein the multiple types of geologic data comprise one of fault geometry data, fracture orientation data, stylolites orientation data, secondary fault plane data, fault throw data, slickenline data, global positioning system (GPS) data, interferometric synthetic aperture radar (InSAR) data, laser ranging data, tilt-meter data, displacement data for a geologic fault, or stress magnitude data for the geologic fault.

[0045] The fault system is segmented into a series of triangulated surfaces using, for example, computer-aided design ("CAD") software. Faults are represented by the triangulated surfaces. The advantage is that three-dimensional fault surfaces more closely approximate curvi-planar surfaces and curved tip-lines without introducing overlaps or gaps. Other known methods of producing triangulated surfaces can be used.

[0046] At 306, for a given triplet among the seven parameters shown in Table 1, the effective shear strain energy is computed using the Mohr-Coulomb criterion. In order to visualize the transition between slip and no-slip, the attribute slip/no-slip is calculated for a variety of values

of (for example) friction, cohesion, orientation of the far field stress. The slip/no-slip attribute corresponds to $W_{eff=0}$ that is computed for each point of the cube. The effective shear strain energy (W_{eff}) is calculated, and the slip-no-slip transition corresponds to the transition $W_{eff}=0$ and $W_{eff}\neq0$. Three variables are chosen in order to display in 3D the rupture envelopes inside a cube. In the description and figures that follow, the three variables are friction, cohesion, stress ratio for the 3 axis (first cube in figure examples), and friction, cohesion and orientation of σ_H for the second cube. For a given fault system made of triangulated surfaces, and for a given triplet (μ, C_o, \overline{R}) , the effective shear stress is computed for each triangle using the Mohr-Coulomb criterion.

[0047] The Mohr-Coulomb criterion is given by $M_c = \mu \sigma_n + C_o$, where μ is the friction coefficient, σ_n is the normal stress on the triangular element and C_o is the cohesion. FIG. 4 show an example representation of a plane with its normal \bar{n} . Here, the traction vector, which is the projection of the stress tensor onto a plane (onto a triangular element) using the Cauchy formula: $t = \sigma \cdot n$, where n is the normal to the triangular element, is $t = \sigma \bar{n}$, where σ is the stress tensor. $\bar{\sigma}_n$ and $\bar{\tau}$ are the projection of t along \bar{n} and on the plane, respectively. σ_n and τ are given by are the projection of the stress tensor on the crack plane and the normal of the plane, respectively and is given by the Cauchy formula:

$$\begin{cases} \sigma_n = (\boldsymbol{\sigma} \bar{\boldsymbol{n}}).\bar{\boldsymbol{n}} \\ \tau = \|(\boldsymbol{\sigma} \bar{\boldsymbol{n}}) \quad [(\boldsymbol{\sigma} \bar{\boldsymbol{n}}).\bar{\boldsymbol{n}}]\bar{\boldsymbol{n}}\| \end{cases}$$

where "." is the inner product, σ is the stress tensor and \bar{n} is the normal to the triangular element. A triangular element, given by its normal \bar{n} , will slip if the shear stress τ is greater or equals to M_c . In such case, the effective shear stress is defined as $\tau_{eff} = \tau$ M_c , and the corresponding shear strain energy for this triangular element is $W_e = a. \tau_{eff}^2$, where a is a constant which depends on the material (taken equal to 1).

[0048] At 308, the sum of the strain energies is computed for all triangles, giving rise to $W_{eff} = a \sum \tau_{eff}^2$. This process is repeated for many values of (μ, C_o, \overline{R}) . At 310, a determination is made as to whether the cube is filled. If not, additional calculations are made at 306 and 308. If the cube is filled, then the method progresses to 312, where, iso-surfaces of W_{eff} are extracted from the cube to display the rupture envelopes for specific values of W_{eff} at 314. Each axis of the cube represents a variable and the three variables (axis) are varied by an increment, and for

8

each value of the tuple (one point of the cube), the W_{eff} is computed. This is done for the whole cube. Filling cube means that we have initially 3 variables (representing the 3 axis of a cube) that are varied from a minimum value to a maximum value with a given step. For each point of the cube (i.e., for each value of the 3 variables), W_{eff} is computed and set the resulting value at that point. This is done for all points of the cube = the cube is filled = all points of the cube have a compute W_{eff} .

[0049] In order to have the effective shear strain energy W_{eff} , one must sum up τ_{eff} for all triangular element making the fault system:

$$W_{eff} = a \sum_{i=1}^{n} \tau_{eff}^{(i)}$$

where a is a constant for the given fault system and which depends also on the mechanical properties, for example, Young modulus, poisson's ratio, density, etc., of the rocks in which the fault system is embedded. From the cube, and for different values of W_{eff} , iso-surfaces are extracted, for example, using a marching cube as the cube is regular. As known in the art, a marching cube is an algorithm for extracting a polygonal mesh of an iso-surface from a three-dimensional discrete scalar field (sometimes called voxels). For a value of W_{eff} close to zero, this corresponds to the transition slip/no-slip. For other values of W_{eff} , this corresponds to a specific property of a fault system, such as the fault system reactivation. The method can end at 316.

[0050] The above method can be represented by an algorithm as follows:

Input:

- 1. Fault system as triangulated surfaces in 3D
- 2. Variable for the X-axis (for example, cohesion C_o)
- 3. Variable for the Y-axis (for example, stress ratio \overline{R} , or the orientation of σ_H , θ)
- 4. Variable for the Z-axis (for example, friction μ)

Filling the cube

```
For C_o varies

For \theta varies

For \mu varies

Let W_{eff} = 0

For each triangle with normal n

Compute \tau and \sigma_n

Compute M_c

If \tau \geq M_c
```

$$\tau_{eff} = \tau \quad M_c$$

$$W_{eff} = W_{eff} + \tau_{eff}^2$$

EndIf

EndFor

Set the value at (C_o, \overline{R}, μ) in the cube to W_{eff}

EndFor

EndFor

EndFor

[0051] FIG. 5 shows graphical convention used for the examples that follow. The rupture envelopes are shown using a coordinate system with axes of the triplet (μ, C_o, \overline{R}) and the triplet $(\mu, C_o, \overline{\theta})$, where $\overline{R} \in [0,3]$, $\overline{R} \in [0,1]$: Normal fault regime, $\overline{R} \in [0,2]$: Strike-slip fault regime, $\overline{R} \in [2,3]$: Thrust fault regime, $\theta \in [0,180]$, $C_0 \in [0,1/2]$, $\overline{\mu} \in [0,1]$, iso-surfaces are W_{eff} , and iso-contours are z. Each cube is 51 x 51 x 51 points.

[0052] FIGS. 6A and 6B illustrate an example rupture envelope for a planar fault and associated triangulated surface, respectively. FIGS. 7A and 7B illustrate an example rupture envelope for a spherical fault and associated triangulated surface, respectively. FIGS. 8A and 8B illustrate an example rupture envelope for two branching faults at 30° and associated triangulated surface, respectively. FIGS. 9A and 9B illustrate an example rupture envelope for two branching faults at 90° and associated triangulated surface, respectively. FIGS. 10A and 10B illustrate an example rupture envelope for two branching faults at 120° and associated triangulated surface, respectively. FIGS. 11A and 11B illustrate an example rupture envelope for salt domes and associated triangulated surface, respectively. FIGS. 12A and 12B illustrate an example rupture envelope for a complex fault system and associated triangulated surface, respectively. FIGS. 13A and 13B illustrate an example rupture envelope for another complex fault system and associated triangulated surface, respectively.

[0053] The foregoing description, for purpose of explanation, has been described with reference to specific embodiments. However, the illustrative discussions above are not intended to be exhaustive or to limit the invention to the precise forms disclosed. Many modifications and variations are possible in view of the above teachings. Moreover, the order in which the elements of the methods described herein are illustrate and described may be re-arranged, and/or two or more elements may occur simultaneously. The embodiments were chosen and described in order to best explain the principals of the invention and its practical applications, to thereby enable others skilled in the art to best utilize the invention and various embodiments with various

modifications as are suited to the particular use contemplated. Additional information supporting the disclosure is contained in the appendix attached hereto.

CLAIMS

What is claimed is:

1. A method for determining rupture envelopes for a fault system, the method comprising: obtaining a representation that depicts one or more faults in a region of the earth as triangulated surfaces;

selecting variables from among parameters comprising stress ratio, orientation of far field stress maximum principal stress, intermediate principal stress, minimum principal stress for the far field stress, and sliding friction and cohesion of the fault system;

determining a strain energy of a triangular element based on a friction coefficient, a normal stress on the triangular element, and a cohesion for the variables;

summing the strain energy of each triangle in the triangulated surfaces to yield an effective shear strain energy;

extracting one or more iso-surfaces of the effective shear strain energy based on the summing; and

creating one or more rupture envelopes for specific values of the effective shear strain energy based on the extracting.

- 2. The method of any preceding claim, wherein the representation is a three-dimensional representation and wherein the variables comprises a triplet of variables.
- 3. The method of any preceding claim, wherein determining the strain energy of the triangular element comprises using a Mohr-Coulomb criterion given by the equation $\mu\sigma_n + C_0$, wherein μ is the friction coefficient, σ_n normal stress on a triangular element, and C_0 is the cohesion.
- 4. The method of any preceding claim, wherein the effective shear strain energy of a value close to zero corresponds to a transition between slip and no-slip for a fault.

5. The method of any preceding claim, wherein the strain energy is based on difference between a projection of a stress tensor on a crack plane (" τ ") and a Mohr-Coulomb criterion, if the τ is greater than the Mohr-Coulomb criterion.

- 6. The method of any preceding claim, wherein the effective shear strain energy is the sum from all triangular elements of the individual strain energy.
- 7. The method of any preceding claim, wherein a transition between slip and no-slip for a fault is characterized by a transition between the effective shear strain energy between zero and non-zero.
- 8. A non-transitory computer-readable medium storing instructions that, when executed by at least one processor of a computing system, cause the computing system to perform a method according to any of the previous claims.
- 9. A computing system comprising:

one or more processors; and

a memory system comprising one or more non-transitory computer-readable media storing instructions that, when executed by at least one of the one or more processors, cause the computing system to perform operations for determining rupture envelopes for a fault system, the operations comprising:

obtaining a representation that depicts one or more faults in a region of the earth as triangulated surfaces;

selecting variables from among parameters comprising stress ratio, orientation of far field stress maximum principal stress, intermediate principal stress, minimum principal stress for the far field stress, and sliding friction and cohesion of the fault system;

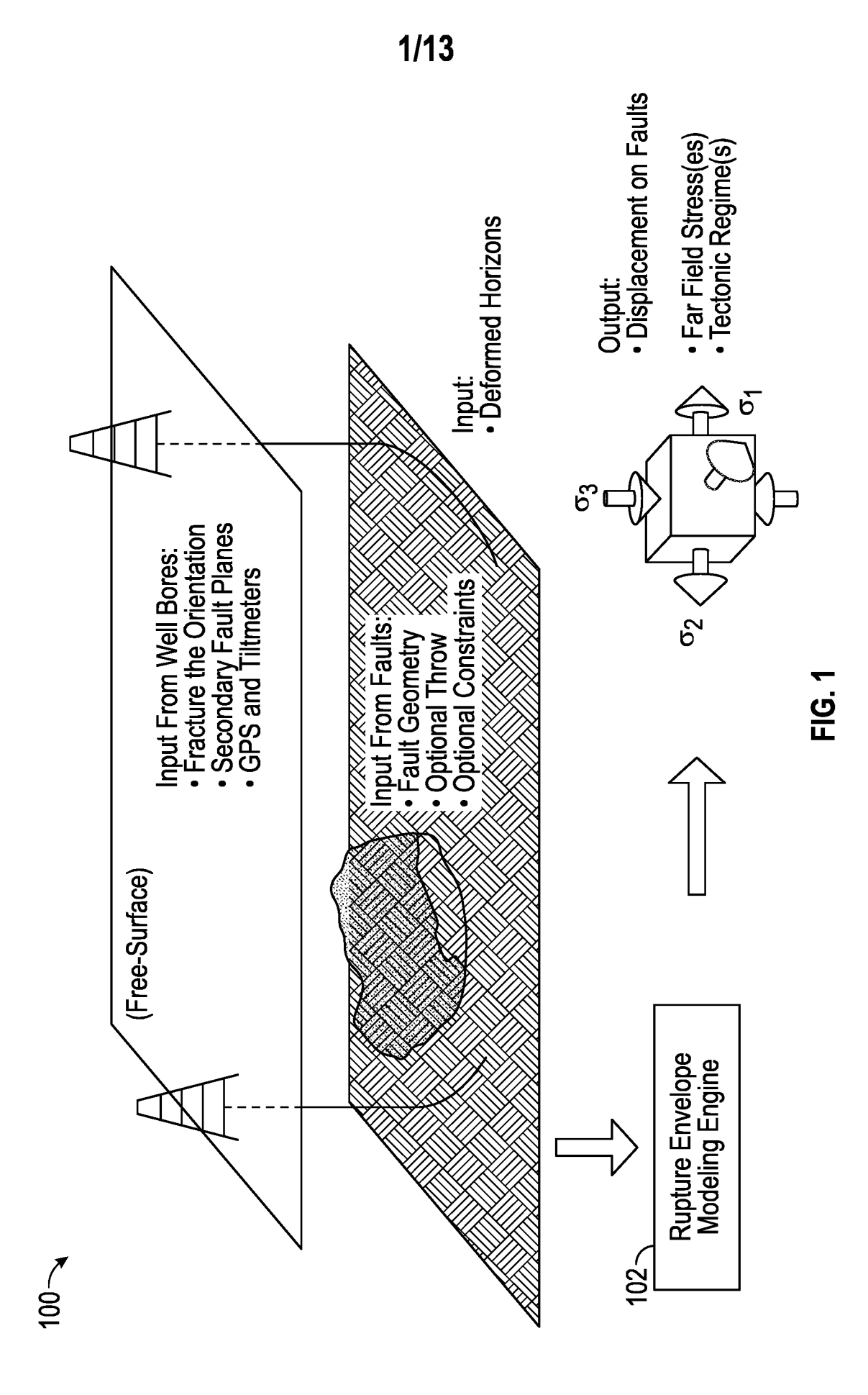
determining a strain energy of a triangular element based on a friction coefficient, a normal stress on the triangular element, and a cohesion for the variables;

summing the strain energy of each triangle in the triangulated surfaces to yield an effective shear strain energy;

extracting one or more iso-surfaces of the effective shear strain energy based on the summing; and

creating one or more rupture envelopes for specific values of the effective shear strain energy based on the extracting.

- 10. The computing system of claim 9, wherein the representation is a three-dimensional representation and wherein the variables comprises a triplet of variables.
- 11. The computing system of claim 9 or claim 10, wherein determining the strain energy of the triangular element comprises using a Mohr-Coulomb criterion given by the equation $\mu\sigma_n + C_0$, wherein μ is the friction coefficient, σ_n normal stress on a triangular element, and C_0 is the cohesion.
- 12. The computing system of any of claims 9-11, wherein the effective shear strain energy of a value close to zero corresponds to a transition between slip and no-slip for a fault.
- 13. The computing system of any of claims 9-12, wherein the strain energy is based on difference between a projection of a stress tensor on a crack plane (" τ ") and a Mohr-Coulomb criterion, if the τ is greater than the Mohr-Coulomb criterion.
- 14. The computing system of any of claims 9-13, wherein a transition between slip and noslip for a fault is characterized by a transition between the effective shear strain energy between zero and non-zero.
- 15. The computing system of any of claims 9-14, wherein the effective shear strain energy is the sum from all triangular elements of the individual strain energy.



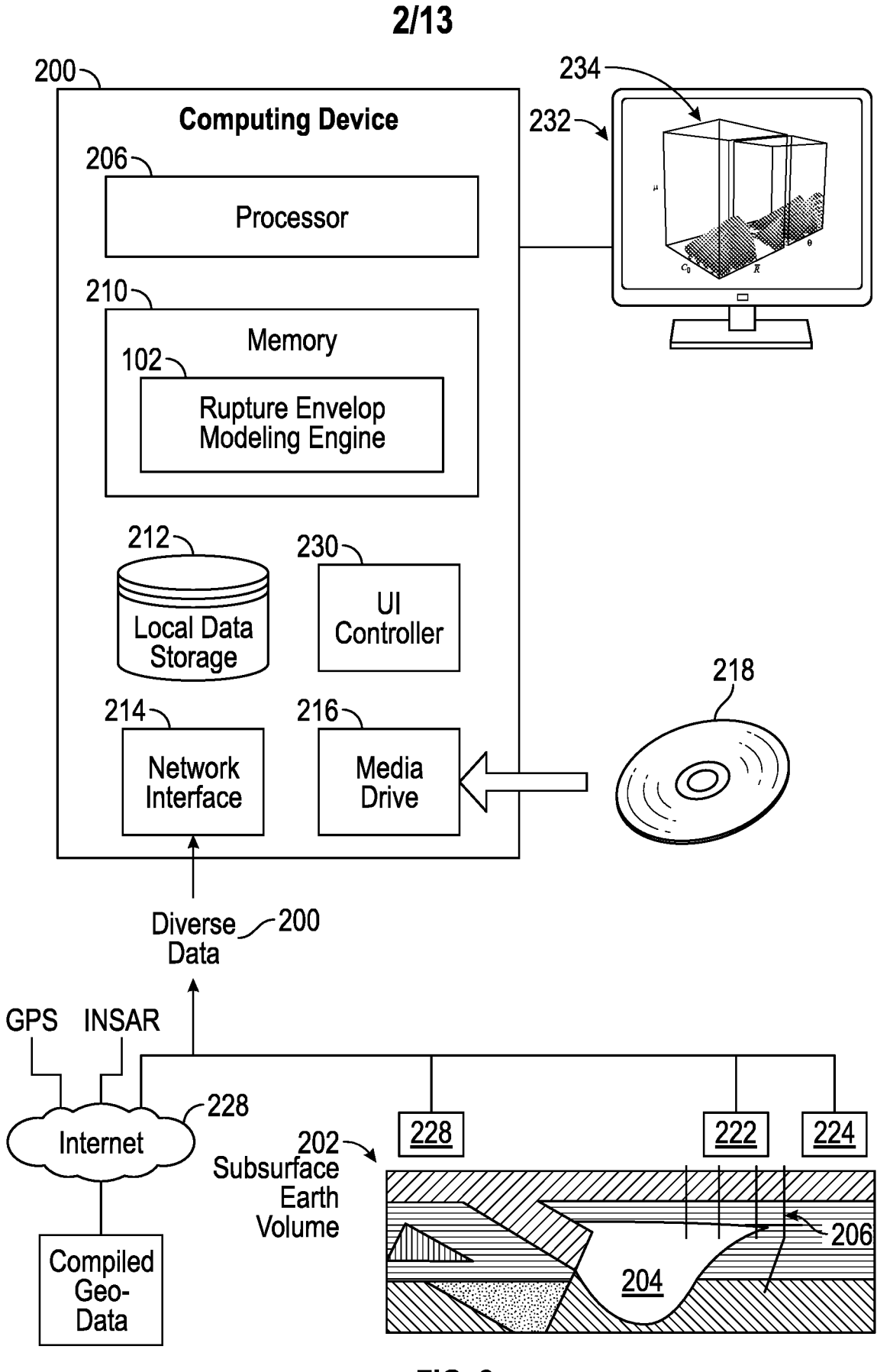
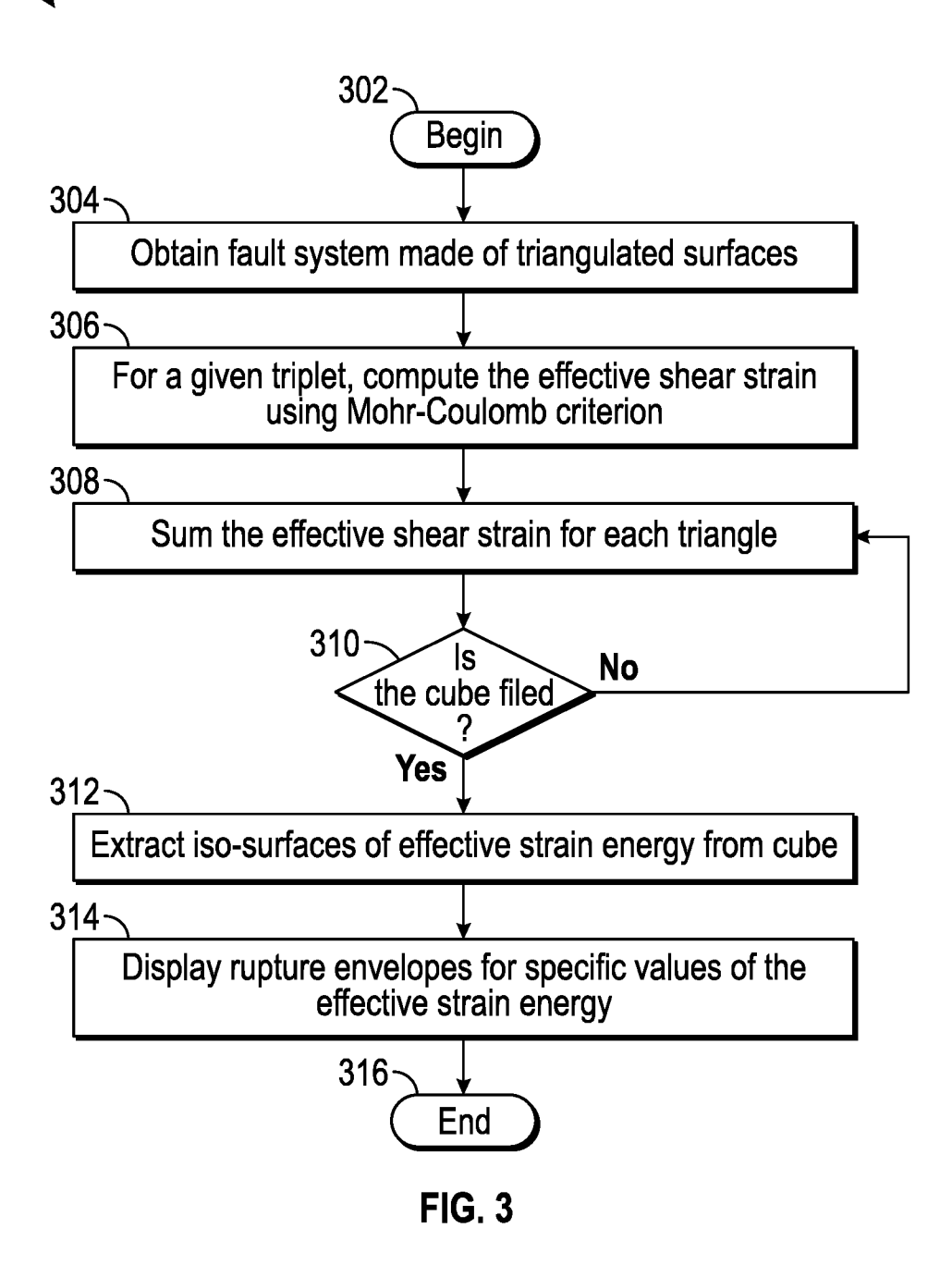


FIG. 2

3/13

300



4/13

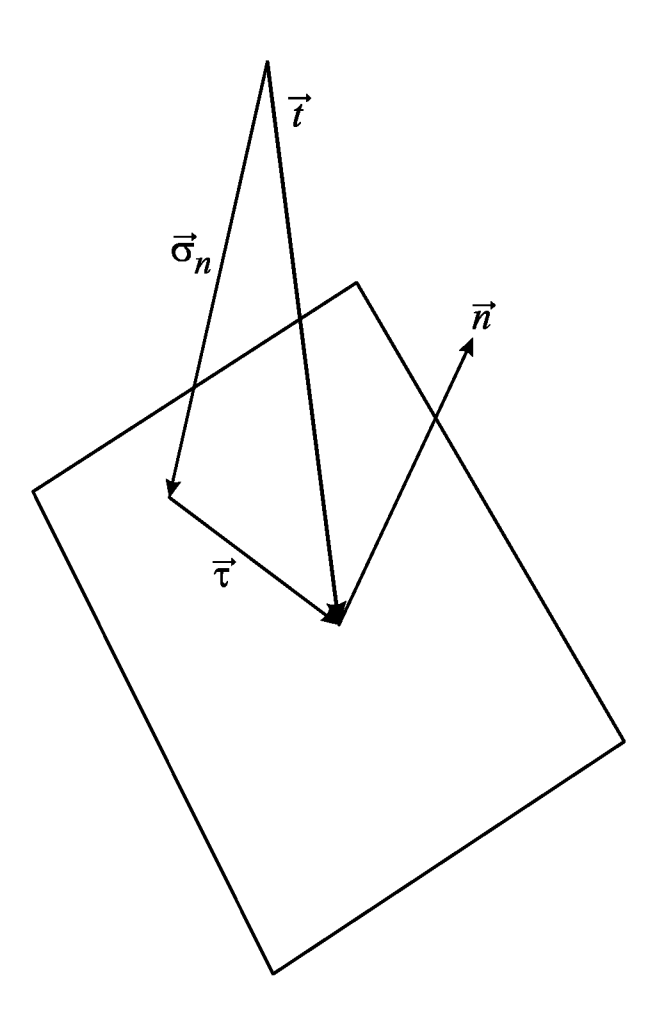
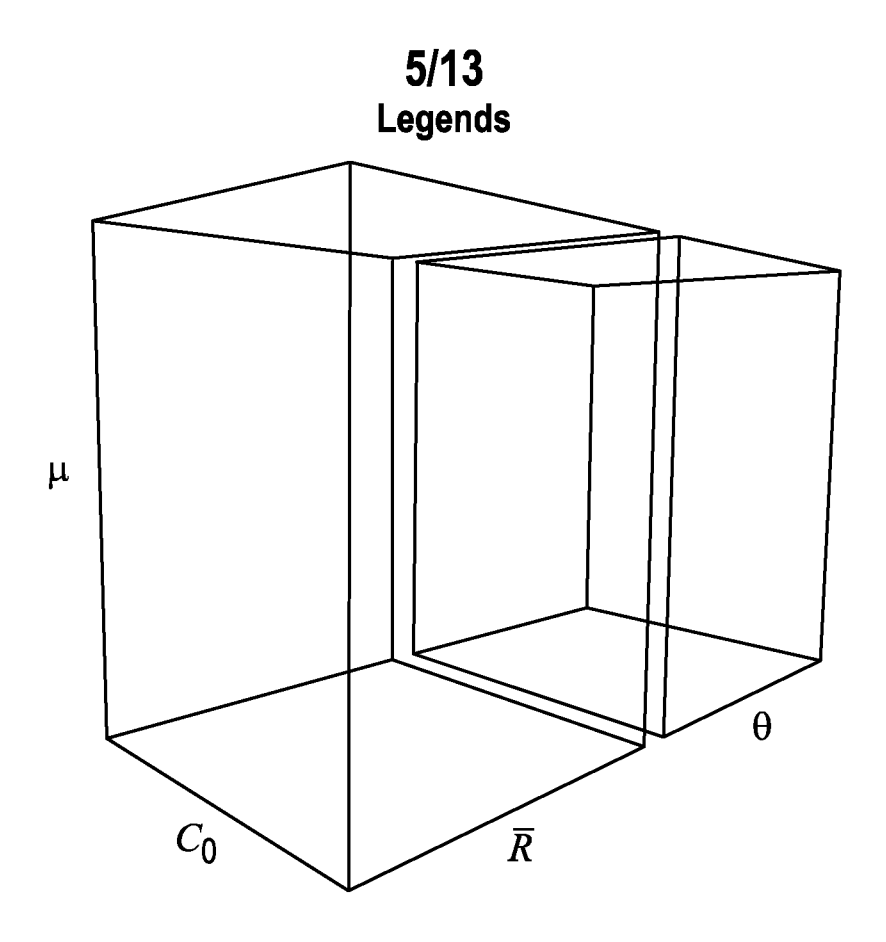


FIG. 4



$\overline{R} \in [0,3]$

 $\rightarrow \overline{R} \in [0,1]$: Normal Fault Regime

 $\rightarrow \overline{R} \in [0,2]$: Strike-Slip Fault Regime

 $\rightarrow \overline{R} \in [2,3]$: Thrust Fault Regime

 $\theta \in [0,180]$

 $C_0 \in [0, \frac{1}{2}]$ $\mu \in [0, 1]$

Iso-Surfaces: W_{eff} Iso-Contours: z

Each Cube is 51 x 51 x 51 Points

FIG. 5

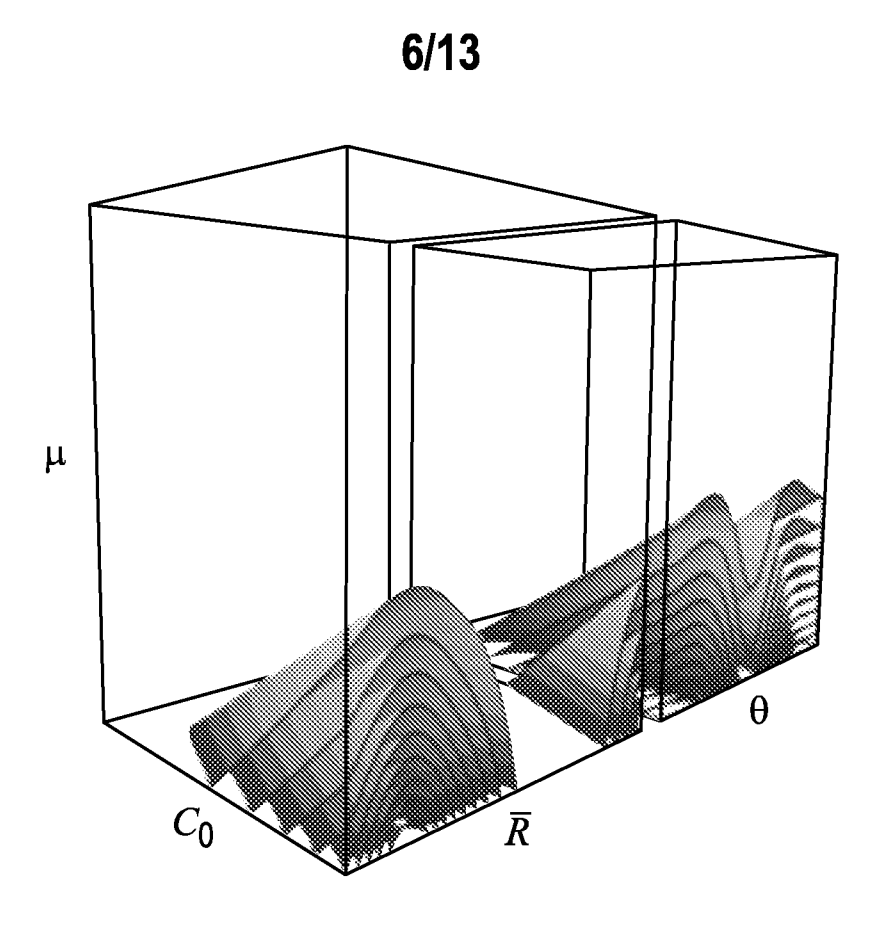


FIG. 6A



FIG. 6B

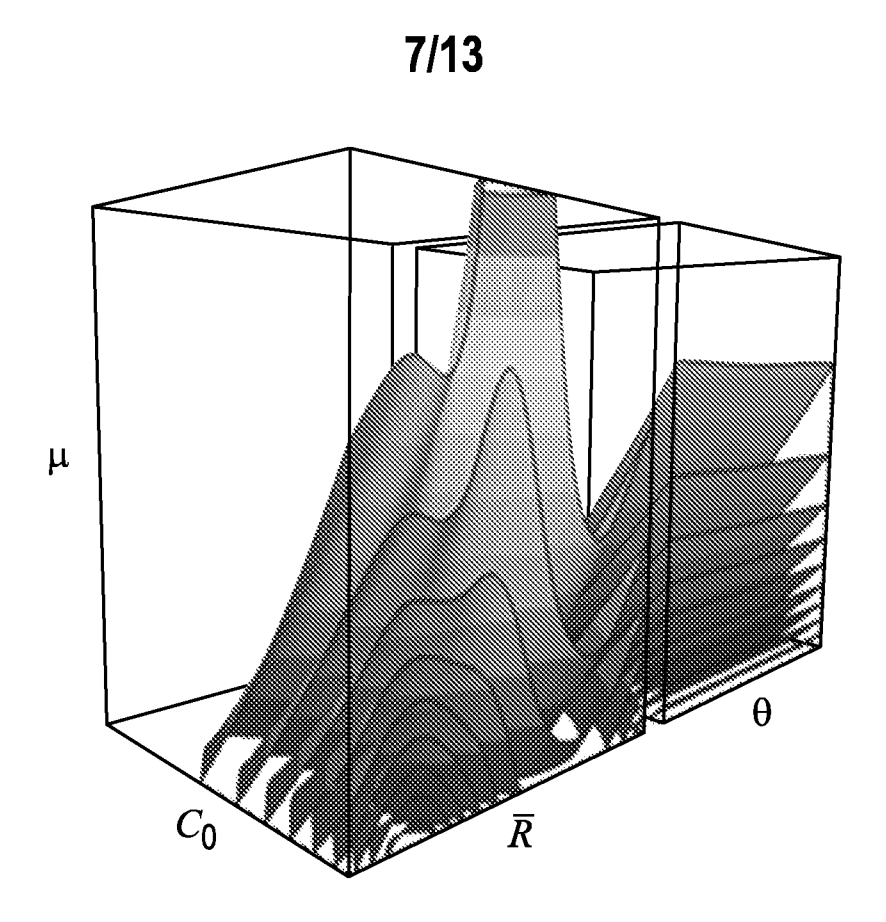


FIG. 7A
Top View

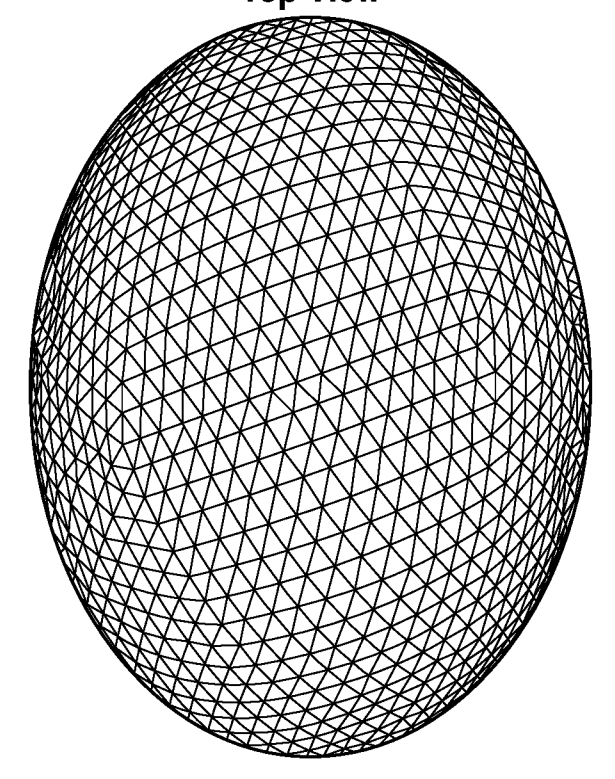


FIG. 7B

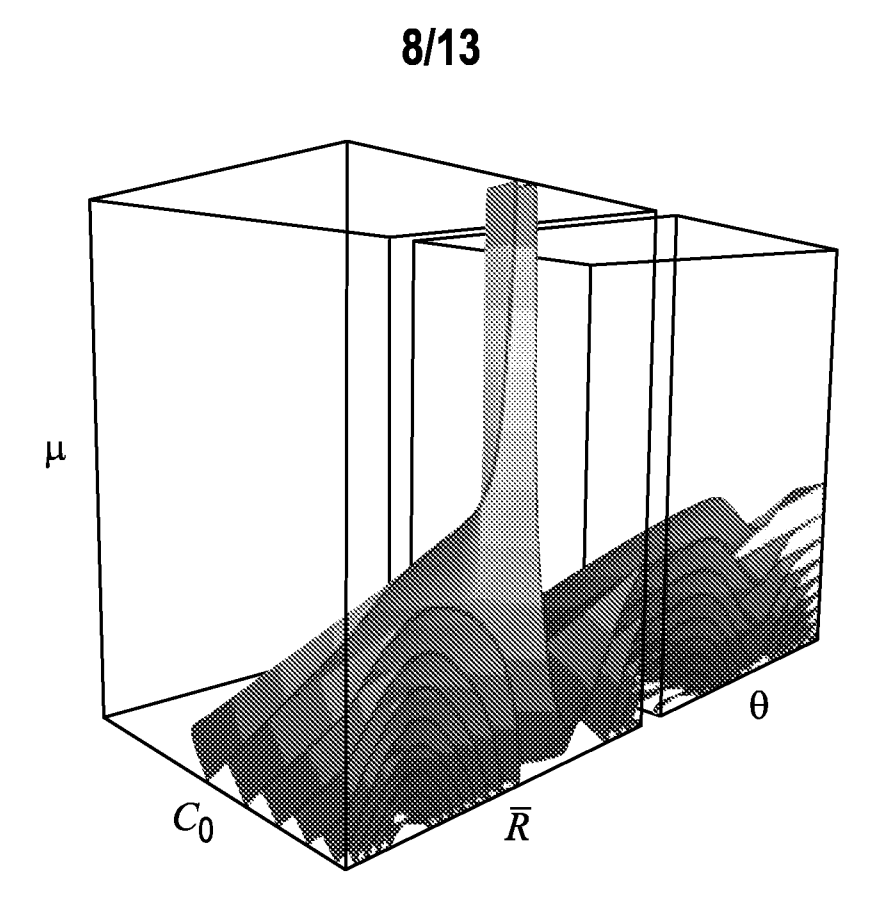


FIG. 8A

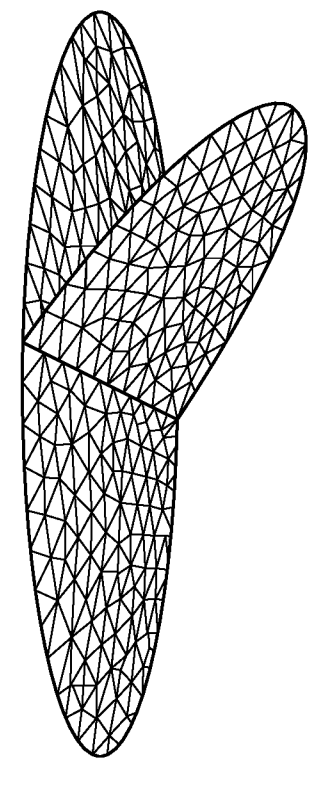


FIG. 8B

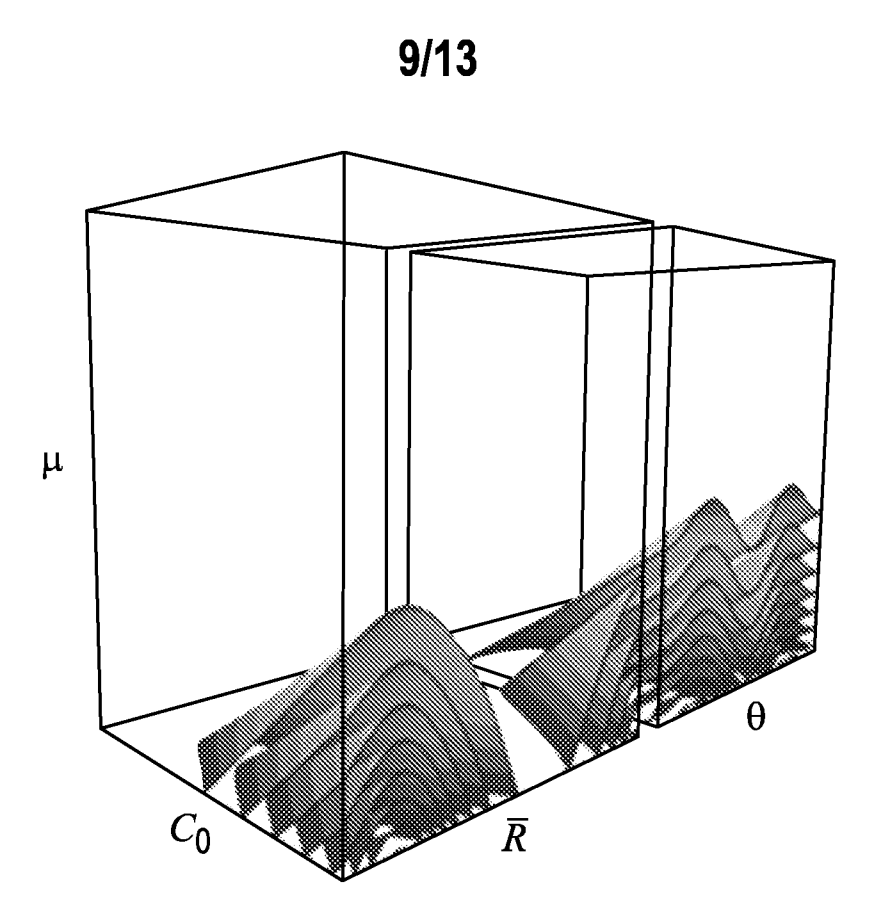


FIG. 9A

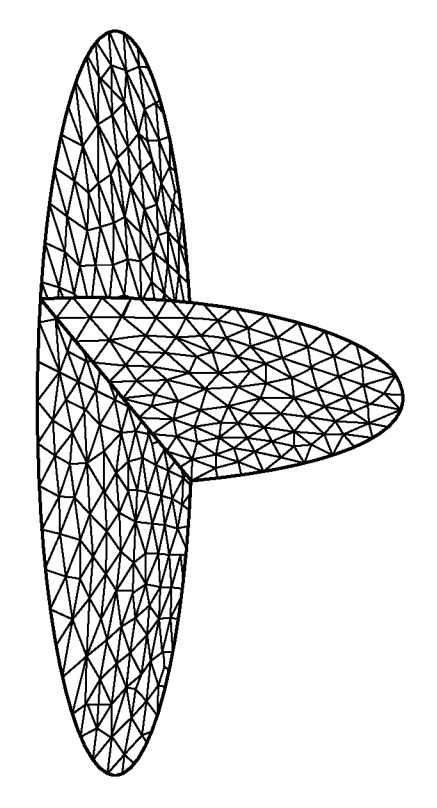


FIG. 9B



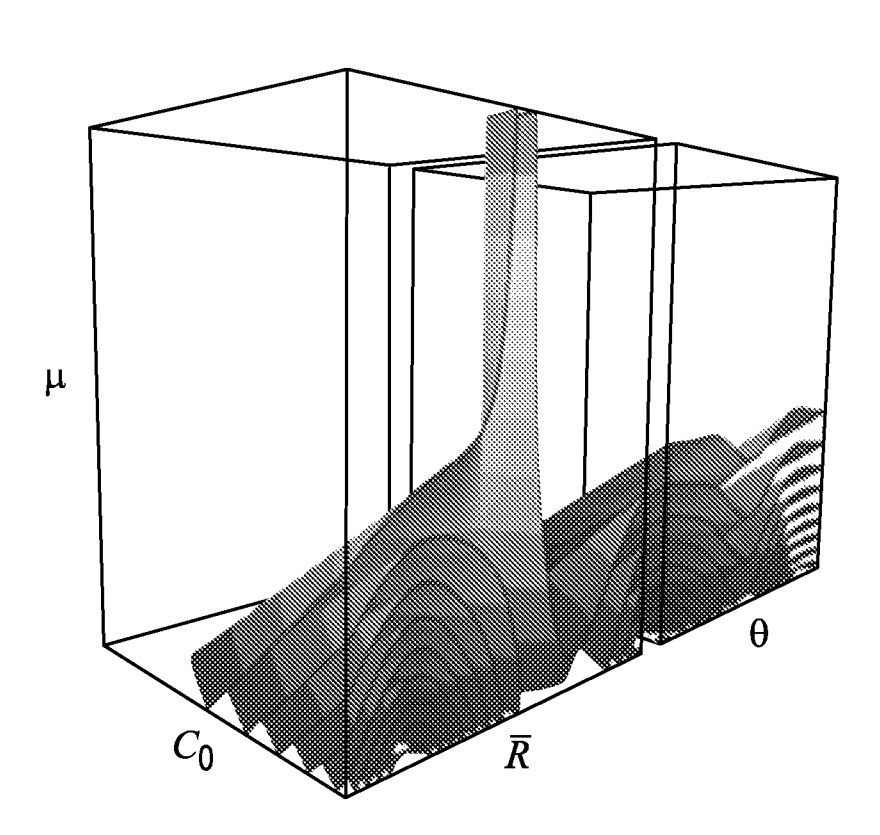


FIG. 10A

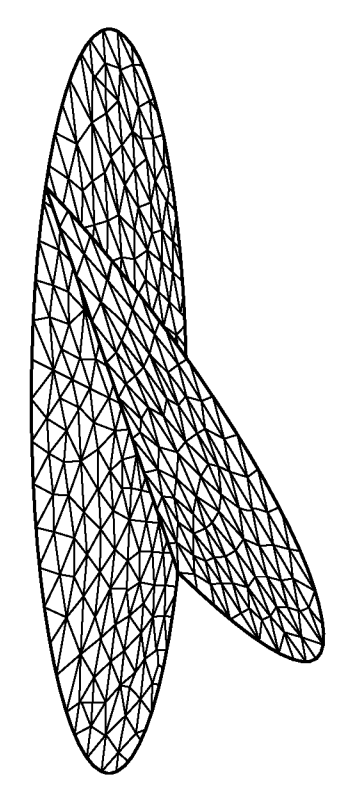
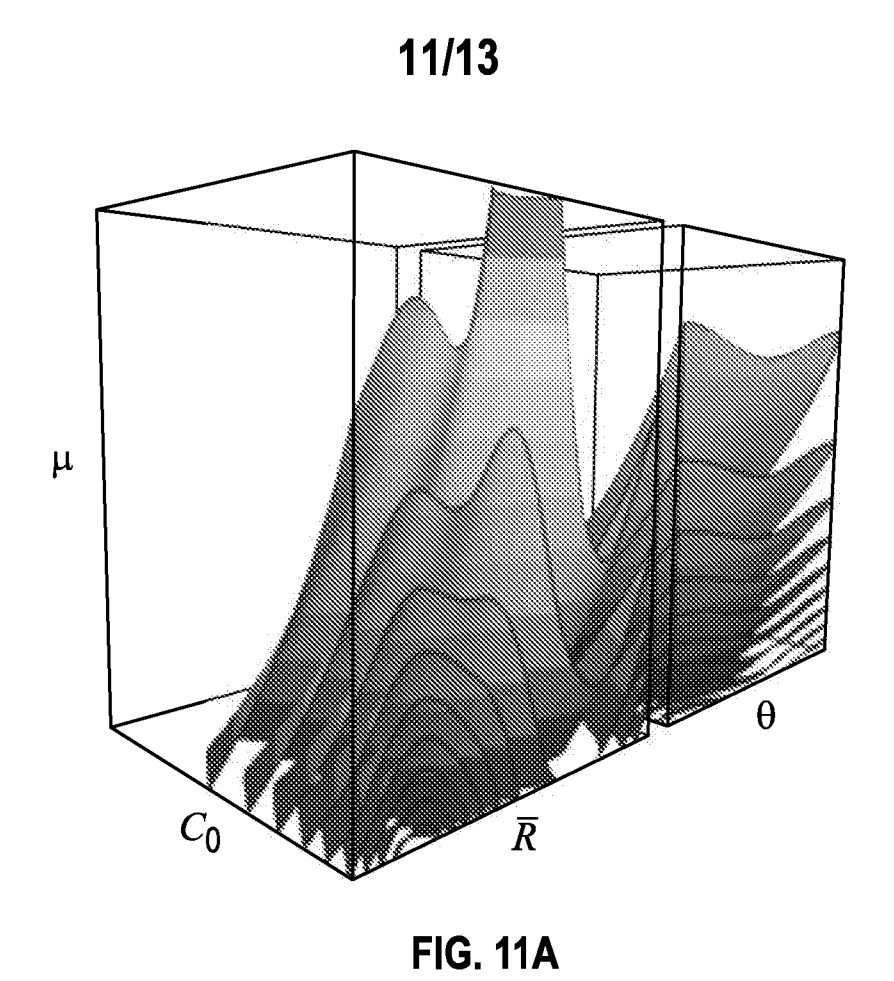


FIG. 10B



Oblique View

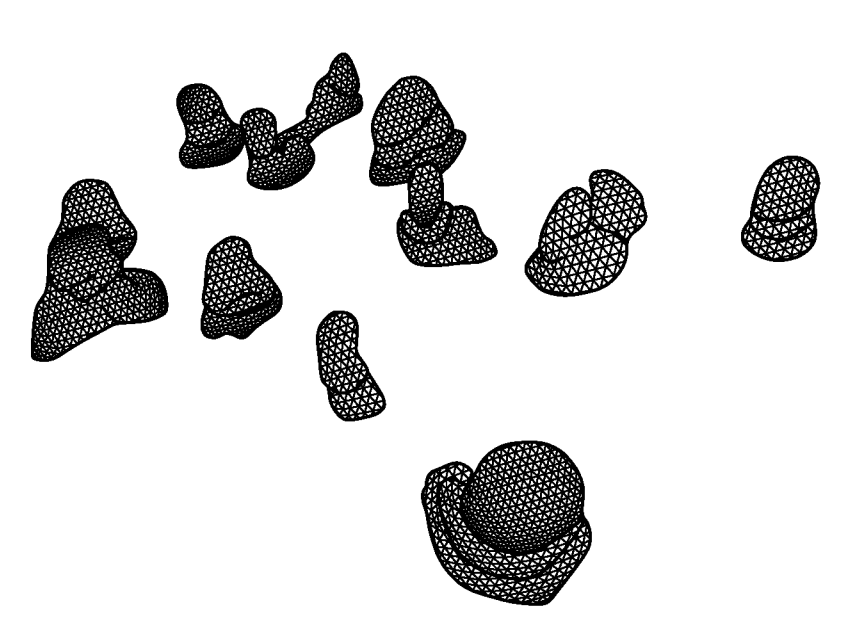


FIG. 11B

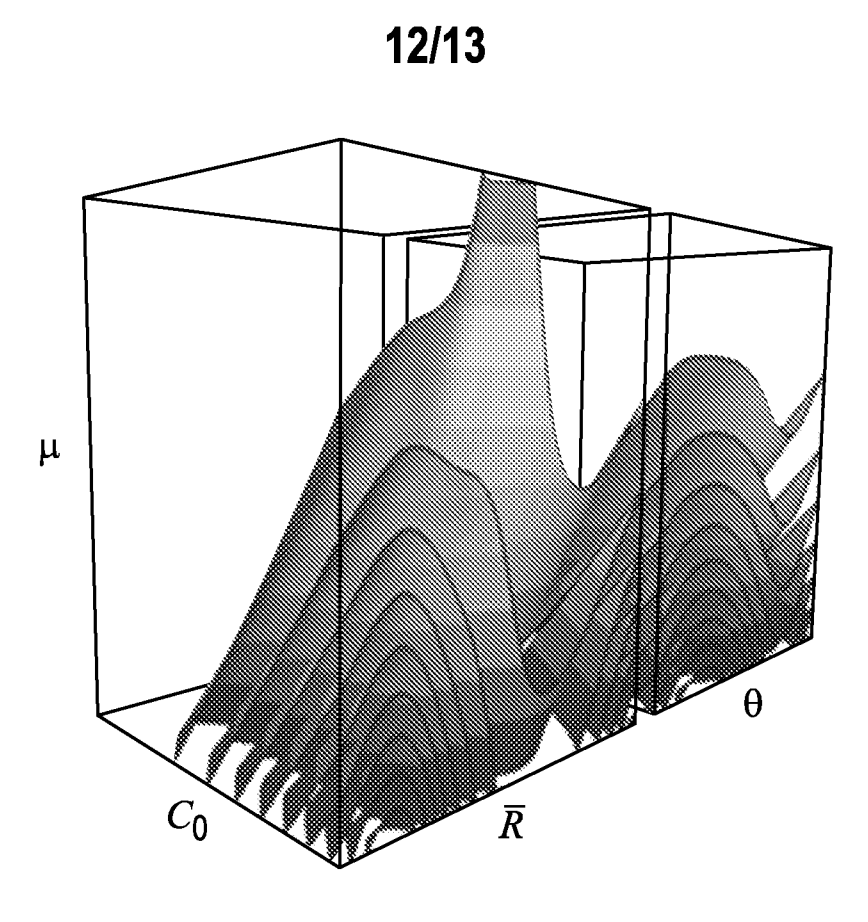


FIG. 12A

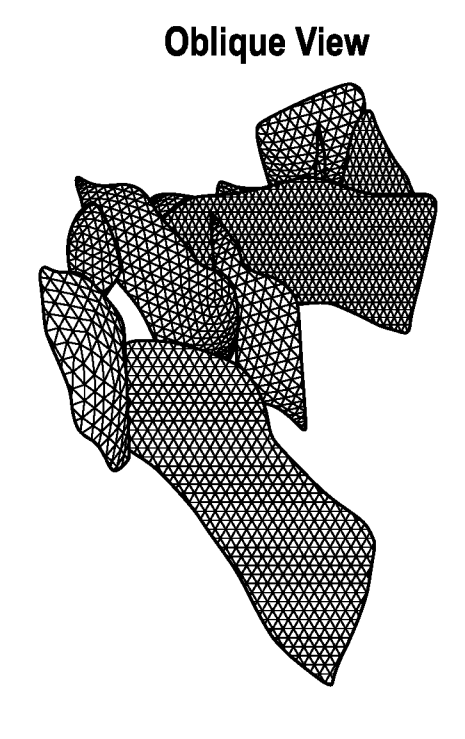


FIG. 12B

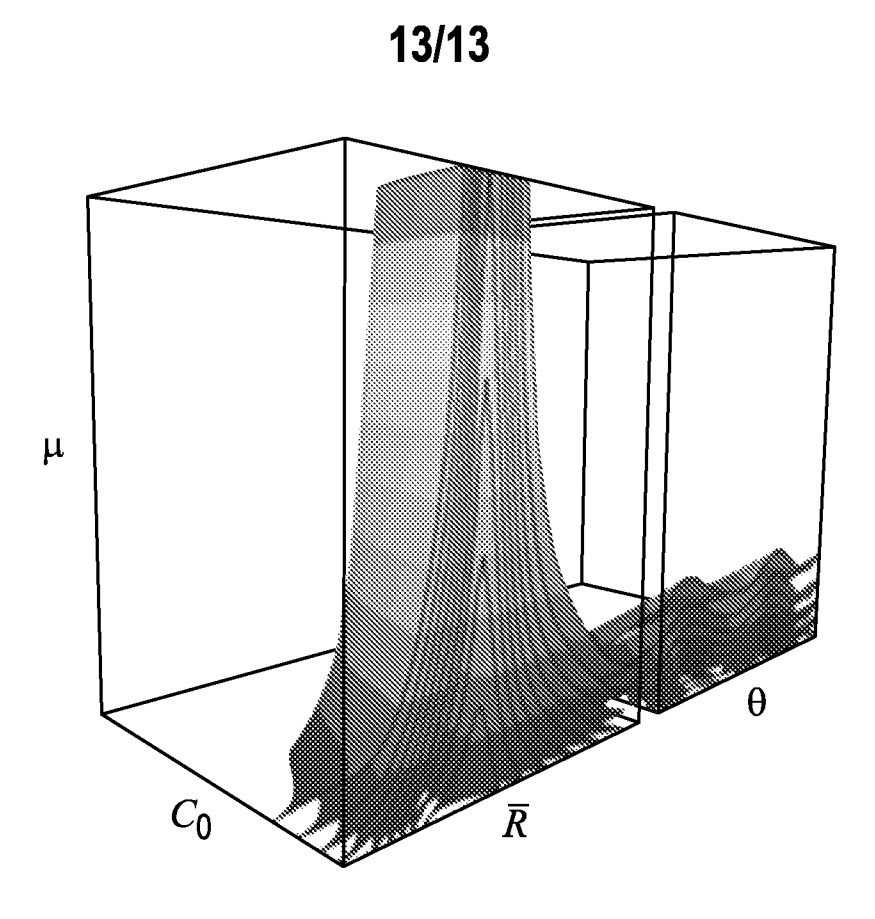


FIG. 13A

Oblique View

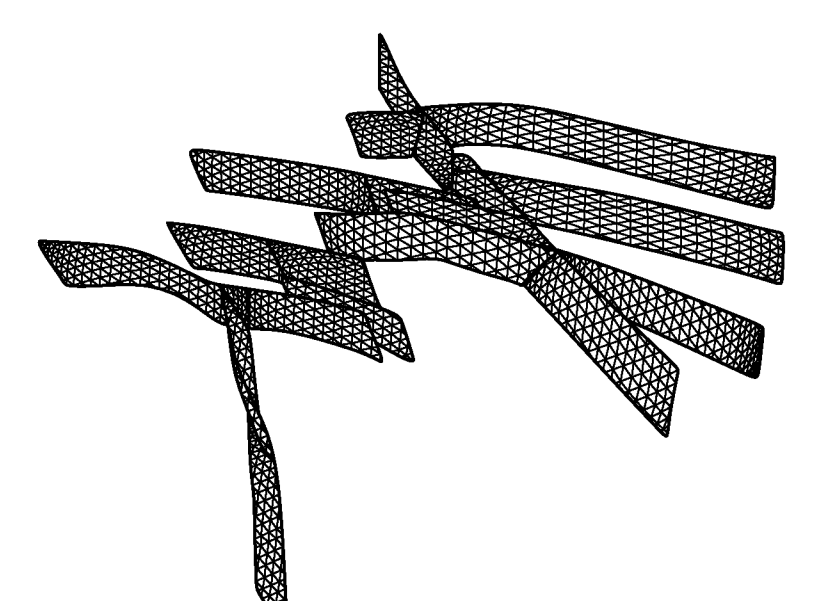


FIG. 13B

INTERNATIONAL SEARCH REPORT

CLASSIFICATION OF SUBJECT MATTER

G01V 1/30(2006.01)i, G01V 1/24(2006.01)i, G01V 1/22(2006.01)i

According to International Patent Classification (IPC) or to both national classification and IPC

FIELDS SEARCHED

Minimum documentation searched (classification system followed by classification symbols) G01V 1/30; G06F 17/10; G06F 17/50; G06G 7/48; G01V 9/00; G01V 1/28; G01V 99/00; G01V 1/00; G01V 1/24; G01V 1/22

Documentation searched other than minimum documentation to the extent that such documents are included in the fields searched Korean utility models and applications for utility models Japanese utility models and applications for utility models

Electronic data base consulted during the international search (name of data base and, where practicable, search terms used) eKOMPASS(KIPO internal) & Keywords: fault, rupture, envelope, parameter, variables, stress ratio, far field stress, principal stress, sliding friction, cohesion, strain energy, iso-surface, triangulated surface, shear strain, normal stress

DOCUMENTS CONSIDERED TO BE RELEVANT

Category*	Citation of document, with indication, where appropriate, of the relevant passages	Relevant to claim No.
A	US 2016-0011333 A1 (SCHLUMBERGER TECHNOLOGY CORPORATION) 14 January 2016 See abstract, paragraphs [0005]-[0007], [0092]-[0102], claims 1, 7-8, table 1, and figure 6.	1-15
A	US 2016-0018542 A1 (SCHLUMBERGER TECHNOLOGY CORPORATION) 21 January 2016 See abstract, paragraphs [0022], [0120]-[0135], claim 1, and figures 6-7.	1-15
A	US 2013-0090902 A1 (YAO et al.) 11 April 2013 See abstract, paragraphs [0082]-[0089], claims 1-10, and figure 5.	1-15
A	US 2010-0076738 A1 (DEAN et al.) 25 March 2010 See abstract, paragraphs [0153]-[0164], claim 1, and figure 5.	1-15
A	US 2002-0091502 A1 (MALTHE-SORENSSEN et al.) 11 July 2002 See abstract, paragraphs [0040]-[0046], claim 1, and figure 1.	1-15

	Further documents are listed in the continuation of Box C.	See patent family annex.
*	Special categories of cited documents:	"T" later document published after the international filing date or priority
"A"	document defining the general state of the art which is not considered	date and not in conflict with the application but cited to understand
	to be of particular relevance	the principle or theory underlying the invention
"E"	earlier application or patent but published on or after the international	"X" document of particular relevance; the claimed invention cannot be
	filing date	considered novel or cannot be considered to involve an inventive
"L"	document which may throw doubts on priority claim(s) or which is	step when the document is taken alone
	cited to establish the publication date of another citation or other	"Y" document of particular relevance; the claimed invention cannot be
	special reason (as specified)	considered to involve an inventive step when the document is
"O"	document referring to an oral disclosure, use, exhibition or other	combined with one or more other such documents, such combination
	means	being obvious to a person skilled in the art
"P"	document published prior to the international filing date but later	"&" document member of the same patent family
	than the priority date claimed	
Date	of the actual completion of the international search	Date of mailing of the international search report
	17 May 2017 (17.05.2017)	17 May 2017 (17.05.2017)

Name and mailing address of the ISA/KR Authorized officer International Application Division

Korean Intellectual Property Office 189 Cheongsa-ro, Seo-gu, Daejeon, 35208, Republic of Korea Facsimile No. +82-42-481-8578

KIM, Jin Ho

Telephone No. +82-42-481-8699



INTERNATIONAL SEARCH REPORT

Information on patent family members

International application No.

PCT/US2017/017082

Patent document cited in search report	Publication date	Patent family member(s)	Publication date
US 2016-0011333 A1	14/01/2016	CA 2896683 A1 EP 2966602 A1 FR 3023641 A1	11/01/2016 13/01/2016 15/01/2016
US 2016-0018542 A1	21/01/2016	CA 2897304 A1 EP 2975437 A1 FR 3023954 A1	15/01/2016 20/01/2016 22/01/2016
US 2013-0090902 A1	11/04/2013	US 9305121 B2 WO 2012-003027 A1	05/04/2016 05/01/2012
US 2010-0076738 A1	25/03/2010	AU 2009-293209 A1 AU 2009-293209 B2 BR P10919207 A2 CA 2738122 A1 CN 102203638 A CN 102203638 B EA 201170472 A1 EP 2342668 A2 EP 2342668 A4 US 8204727 B2 WO 2010-033710 A2 WO 2010-033710 A3	25/03/2010 09/07/2015 08/12/2015 25/03/2010 28/09/2011 17/07/2013 31/10/2011 13/07/2011 02/11/2016 19/06/2012 25/03/2010 01/07/2010
US 2002-0091502 A1	11/07/2002	AU 2002-367246 A1 AU 4981501 A1 BR 0109957 A CA 2405308 A1 CA 2405308 C EP 1297411 A1 EP 1297411 A4 MY 134182 A NO 20024762 A NO 331501 B1 OA 13052 A US 2002-0010570 A1 US 2002-0029137 A1 US 2002-0059048 A1 US 6370491 B1 US 7031891 B2 US 7043410 B2 US 7089166 B2 US 7188058 B2 WO 01-75588 A1 WO 02-082352 A1 WO 03-056498 A1	15/07/2003 15/10/2001 27/05/2003 11/10/2001 21/01/2014 02/04/2003 29/12/2010 30/11/2007 28/11/2002 16/01/2012 10/11/2006 24/01/2002 07/03/2002 16/05/2002 09/04/2002 18/04/2006 09/05/2006 08/08/2006 06/03/2007 11/10/2001 17/10/2002 10/07/2003